

# **DIELECTRIC BEHAVIOR OF BIOPOLYMER BASED COMPOSITES CONTAINING MULTI WALL CARBON NANOTUBES: EFFECT OF FILLER CONTENT AND ASPECT RATIO**

**Pellegrino Musto<sup>a</sup>, Pietro Russo<sup>a,\*</sup>, Francesca Cimino<sup>b</sup>, Domenico Acierno<sup>c</sup>,  
Giovanni Lupò<sup>d</sup>, Carlo Petrarca<sup>d</sup>**

<sup>a</sup>*Institute for Polymers, Composites and Biomaterials. National Council of Research of Italy. Via  
Campi Flegrei, 34 – 80072 Pozzuoli (NA), Italy*

<sup>b</sup>*Departments of Chemical, Materials Engineering and Industrial Production. University of  
Naples Federico II. Piazzale Tecchio, 80 – 80125 Naples, Italy*

<sup>c</sup>*INSTM – Reference Centre for Processing Technology of Polymers and Composites. University  
of Naples Federico II. Piazzale Tecchio, 80 – 80125 Naples, Italy.*

<sup>d</sup>*Department of Electrical Engineering and Information Technology. University of Naples  
Federico II. Piazzale Tecchio, 80 – 80125 Naples, Italy*

---

\* Corresponding author. Tel. +39 081 7682268; fax: +39 081 7682404  
E-mail address: [pietro.russo@unina.it](mailto:pietro.russo@unina.it) (P. Russo)

### **Abstract**

Multi wall carbon nanotubes (MWCNTs) with different aspect ratios (30, 105 and 667) were included in a commercial fully biodegradable blend using melt mixing. Samples of composite systems prepared by hot molding and containing up to 1.2 vol% of MWCNTs were studied by means of DC electrical resistivity and dielectric spectroscopy in order to enhance effect of filler content and aspect ratio on their dielectric behaviour. Raman spectroscopic investigations and morphological observations were also performed in order to correlate dielectric behaviour with surface carbon nanotubes features and to check the actual level of dispersion of carbon nanotubes under the applied processing conditions. Results emphasized that the carbon nanotubes aspect ratio and their surface regularity determine the electrical properties of composites because they strongly influence percolation thresholds, dielectric permittivity and dissipation factor of produced materials. A satisfying dispersion of the filler seems to be achieved under the employed processing conditions. These preliminary results demonstrates possible applications of this type of biobased systems in many applications going from stress control to devices for high storage energy.

**Keywords:** Biocomposites, multiwall carbon nanotubes, aspect ratio, dielectric properties

## 1. Introduction

Recently, the growing awareness about finite petroleum resources and significant environmental impact of plastic items at the end of their useful life have justified a huge amount of research efforts reported in the literature about bio-based materials. The general interest of academic and industrial researchers is to exploit potentialities of the so-called biopolymers, intrinsically biodegradable or derived from renewable resources.

Currently environmentally friendly resins are already applied in various fields as biomedical, food packaging and coating ones. However, limitations essentially in terms of their high cost and inferior physical properties with respect to traditional petroleum based plastics still restrict their potential spectra of industrial applications. In this frame, several researches have been focused on specific methodologies aimed to improve functional properties of commercial available biopolymers as poly(lactic acid) (PLA) [1,2], poly(hydroxy alkanates) (PHA) [3,4] and polycaprolactones (PCL) [5,6].

Common routes to achieve valuable targets are the inclusion of nanometric fillers or the blending with other resins, preferably biobased ones, in order to obtain new fully eco-sustainable products. About the first approach, usually the inclusion of rigid nanosized fillers not only improves mechanical properties of the host matrix but also it may enhance specific functional properties of the same. For example, it is well known that carbon nanotubes are promising reinforcing filler for polymers due to their excellent mechanical, electrical and thermal properties.

As far as blending is concerned, appropriate choices in terms of second organic phase, composition, operative conditions and even the inclusion of nanofillers may give rise to co-continuous morphologies, responsible of synergistic interactions between the phases mixed together and products with very interesting performances [7,8]. This is the case of the blend considered in this study, constituted by two semicrystalline co-polymers, poly(hydroxyl butyrate-co-valerate) (PHBV) and poly(butylenes adipate-co-terephthalate) (PBAT), and commercially available as a film grade resin with a weight ratio 30/70, respectively. In fact, although PHBV copolymers are among the most studied PHA resins, their applications are limited by some drawbacks as slow crystallization rate, very high crystallinity, brittleness, relatively difficult processing due to the low melt viscosity and small processing window. PBAT

co-polymers, with their high flexibility and processability, are potential candidates to improve properties of PHBV resins and retain biodegradability of products.

In this work, specific interest is dedicated to the improvement of the dielectric behavior of this blend in order to extend its potential use [9, 10], focusing the attention on the effect of filler content and aspect ratio [ $\eta$ ]: geometrical parameter affecting, as well established, percolation thresholds and, consequently, physical properties of final products [11, 12].

Electrical resistivity (conductivity) of polymer composites containing carbon nanotubes of different type (single, double, multi wall), synthesis method, treatment, manufacturer and aspect ratio have been extensively studied [13]; a wide range of resistivity values has been reported but a comparison among different data can be still very difficult. Fewer results are available on biodegradable composites, as for instance on polyvinyl alcohol PVA [14] or poly(L-lactide) PLLA [15], which are becoming of increasing interest for many electrical and electronic devices.

At this purpose, systems containing low amounts of multiwalled carbon nanotubes were prepared by melt compounding and analyzed in terms of thermal, morphological and dielectric issues. Main results obtained so far allow to foresee interesting perspectives of investigated systems in electric/electronic and storage energy fields.

## **2. Experimental**

### *2.1 Materials*

A commercial PHBV/PBAT blend (named E-PHBV) was purchased in pellet form from Ningbo Tianan Biologic Material Co. Ltd. (Tianan-ENMAT) (China) under the trade name 6010P. The weight ratio between PHBV and PBAT is 30:70.

Multi wall carbon nanotubes (MWCNTs) used as fillers differ essentially in terms of their aspect ratio parameter as clearly highlighted by Table 1 reporting some features of the same.

Prior to melt mixing, the matrix and the fillers were vacuum dried at 70 °C for 12 hours.

**Table 1.**

Information about considered carbon nanotubes.

Trade code	Supplier	Mean outer diameter (nm)	Length ( $\mu\text{m}$ )	Aspect ratio $[\eta]$	True density (g/cc)	Purity (%)
4060	Shenzen Nanotechnologies	50	1,5	30	2,16	> 97%
3150	Nanocyl	9,5	1	105	1,94	> 95 %
724769	Sigma Aldrich	7,5	5	667	2.1	> 95 %

## 2.2 Composite and sample preparation

All formulations containing multi wall carbon nanotubes contents up to 1.5 vol. % were prepared using a HAAKE PolyLab mixer at 175 °C, with a screw speed of 60 rpm and a residence time of 7 min. Systematic thermogravimetric measurements, not shown here, confirmed a good agreement between nominal and actual filler contents.

Samples for DC electrical volume resistivity ( $\rho_v$ ) measurements were obtained by applying a hydraulic pressure of about 2 MPa at 180 °C for two minutes with a compression molding machine (LabTech Engineering, LP20-B). They have a circular shape, with a diameter of about 40 mm and a thickness approximately equal to 1.0 mm.

## 2.3 DC Volume electrical conductivity

Measurements were performed at room temperature by a standard volt-amperometric method by holding each specimen in a shielded cell with guarded ring electrodes. The volume electrical conductivity was estimated on the basis of the quasi-steady state value of the current taken after 180 seconds from the application of a step voltage :

$$I = \frac{U}{R}$$

where  $t$  and  $A$  are the thickness and area of the sample, respectively.

In order to reduce the thermal effects, fields ranging between 0.5 to 1 kV/m were applied to the samples. With the aim of verifying the reproducibility of the measurement, a rigid procedure was also adopted. Prior the electrical measurements, the specimen were conditioned

by keeping them in an oven at the controlled temperature of 40°C for 48 hours. Each sample was then measured four times and, between two consecutive measurements, it was always held between grounded electrodes until the short circuit currents fell below the noise level. Moreover, electrical connections were always removed and then reconnected every time before the application of the step voltage . The measurement system was remotely controlled by a dedicated software in MATLAB® and is composed of a HP4140B picoammeter and a stabilized DC source HP6516A.

Data presented in this article are averaged over at least four measurements taken on separated samples of the same typology. A total number of more than 350 measurements on a large variety of samples were performed and discussed in the following in order to extensively highlight the influence of CNT's volume content (*vol%*) and aspect ratio ( $\eta$ ) on the electrical properties of biodegradable composites.

#### 2.4 Dielectric spectroscopy

AC impedance spectroscopy was performed at room temperature using a standard impedance analyzer HP4192A and a suitable shielded cell Agilent 16451B. The dielectric test fixture was equipped with a four-terminal pair cable assembly and it was used in the guarded electrode configuration. The frequency has been varied in the range [0.1 kHz ÷ 10 MHz]. Also in this case, samples were pre-conditioned in oven and four measurements were taken for each of them. Reported data are again average values of 4 measurements, taken each on four samples of the same typology.

By modeling the complex admittance of the test sample as a parallel ( $G_{eq}$ - $C_{eq}$ ) circuit, the impedance analyzer allows the direct measurement of both the equivalent capacitance  $C_{eq}$  and dissipation factor  $\tan\delta$ . Then, from the geometry of the samples, the real part  $\varepsilon'$  of complex permittivity can be easily calculated as:

—

#### 2.5 Raman spectroscopic analysis

Raman measurements were performed by a Horiba Jobin Yvon spectrometer Mod. Labspec Aramis. A diode laser emitting at 532 nm was used as exciting radiation; the exposure

time was 50 s. The 180° back-scattered emission was collected by an Olympus BX41 optical microscope equipped with an Olympus metallurgical objective (MPlan 50x, NA = 0.75) which allowed to record the visible image of the sample as well.

The spectrometer was operated with a grating of 600 grooves/mm and with confocal and slit apertures both set to 200 μm. The radiation was focused onto a Peltier-cooled CCD detector (Synapse Mod. 354308); data collection was performed in the Raman-shift range 3100 – 100 cm<sup>-1</sup>.

## 2.6 Morphological observations

The morphology of all investigated compounds was analyzed using a scanning electron microscope (SEM, Philips XL 20 Series) at an accelerated voltage of 20 kV. The SEM samples were prepared by cryo-fracturing the compression pressed samples. With the main aim to verify the actual filler dispersion, the fractured surfaces was preliminarily coated with a gold-palladium alloy for better electron discharge and to obtain a good resolution of micrographs.

## 3. Results and discussion

### 3.1 DC Volume electrical conductivity

Remarkable differences have been found in the electrical conductivity of the samples as a function of filler's content and shape. Fig. 1a shows the variation in DC volume conductivity, at different aspect ratios, as a function of the filler loading over a relatively broad range [0.003 - 1.2] vol% of fillers; the volume conductivity of the neat polymer in this study is  $1.5 \cdot 10^{-11}$  S/m.

As expected, we have found that, since MWCNT's are very good conductive fillers, they allow the composite to progressively enhance its conductivity as their concentration increases. When an upper limit (the so-called percolation threshold) is reached, conducting paths are formed and the composite experiences a sudden rise of (almost ten orders of magnitude with respect to the neat polymer). Moreover, we have also found another transition threshold at lower filler concentrations, above which the conductivity can increase of about three orders of magnitude. The way such thresholds are reached and the value of the thresholds are sensibly dependent on the filler's aspect ratio (see Table 2).

In fact, three different trends of  $\sigma$  vs. filler content are visible in Fig. 1a, depending on the aspect ratio of carbon inclusions. As concerns as the case  $\phi = 0.01$ , we can notice a first sudden rise of electrical conductivity (about three orders of magnitude) at extremely low filler content ( $\phi = 0.001$ ); then, conductivity remains almost unchanged until the percolation threshold  $\phi_c$  is reached ( $\sigma$  increases from  $10^{-10}$  to  $10^{-7}$  S/m), as shown in detail in Fig. 1b). Above this critical concentration,  $\sigma$  follows a typical scaling law [13] of the form (Fig. 2a):

In composites containing carbon nanotubes with lower aspect ratio ( $\phi = 0.01$ ), the volume conductivity rises very slowly until the filler content is  $\phi = 0.01$ ; above this value a first sudden increase occurs and  $\sigma$  reaches the value  $10^{-8}$  S/m. By increasing the amount of filler, the conductivity doesn't vary until the percolation threshold  $\phi_c = 0.02$ , above which the conductivity rises from  $10^{-8}$  to  $10^{-7}$  S/m. At higher concentration the conductivity varies according to the power law (Fig. 2b):

characterized by a lower power exponent  $n = 1.5$  with respect to samples with higher aspect ratio, in which  $n = 2.5$ .

In composites formed by nanotubes with  $\phi = 0.01$ , only a gradual increase of conductivity with filler content has been measured. In the chosen range of filler content, percolation does not occur and the maximum value of volume conductivity  $\sigma = 10^{-8}$  S/m is reached at  $\phi = 0.01$ . In this case the conductivity variation follows a double exponential law (Fig. 3):

The results illustrated above show that the aspect ratio is a crucial parameter for the formation of conductive pathways in the polymer matrix. Even the introduction of a small amount of nanofillers can lead to a sensible increase in conductivity, especially in composites containing high aspect ratio nanotubes (i.e.  $\phi = 0.01$ ), which can probably more easily bridge



part of the gap between the electrodes and lead to a partial change of the insulating properties of the composite. The transition threshold becomes greater with nanotubes having  $\eta = 667$  tends to disappear in composites containing fillers with low aspect ratio ( $\eta = 30$ ) in which only a gradual increase in conductivity has been recorded.

As concerns as the percolation threshold, the excluded volume theory [15] predicts its theoretical value as  $\phi_c = \frac{1}{\eta}$ . The measured threshold  $\phi_c$  is equal for both composites containing nanotubes with  $\eta = 667$  and nanotubes with  $\eta = 105$ . The experimental value is in the same order of magnitude of the corresponding theoretical values ( $\phi_c = 0.0015$  and  $\phi_c = 0.0095$ , respectively), although greater for nanotubes with high aspect ratio and smaller for the composites containing nanotubes with lower  $\eta$ . The differences found in our measurement results could be explained by considering that the excluded volume theory is based on a statistical spatial distribution of filler particles, on direct contact between them and on the main assumption of “large” aspect ratios, typically higher than 1000. As a consequence, the theoretical threshold becomes a pure geometrical factor which depends uniquely on the likelihood of contact between neighbors, while in general it can be greatly influenced by factors like the motion of nanoparticles or the quality of their dispersion [16].

Regarding the variation of conductivity above the percolation threshold, the higher power exponent  $n = 1.5$  measured in composites characterized by  $\eta = 667$ , testifies that the adding of high aspect ratio nanotubes promotes the formation of conducting paths.

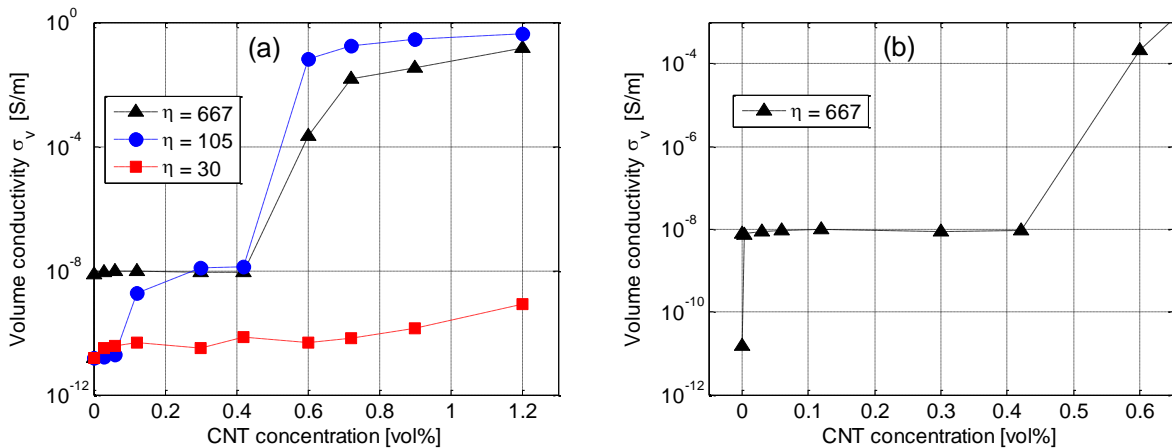


**Fig. 1.** Volume conductivity vs. MWCNT content: comparison among different aspect ratios (a); detail for composites with  $\eta=667$  (b)

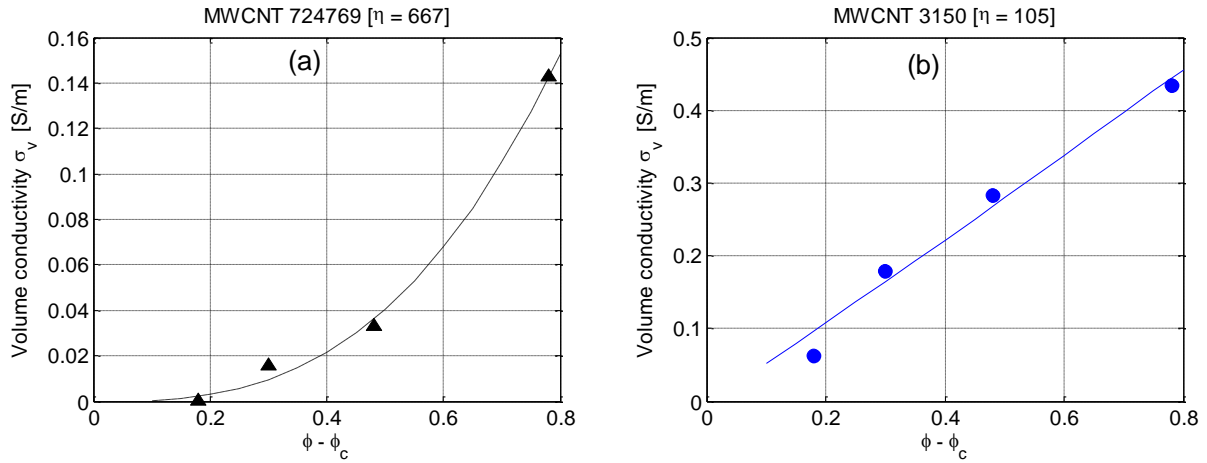


**Fig. 2.** Volume conductivity vs. MWCNT above the percolation threshold; a)  $\eta=105$ ; b)  $\eta=667$

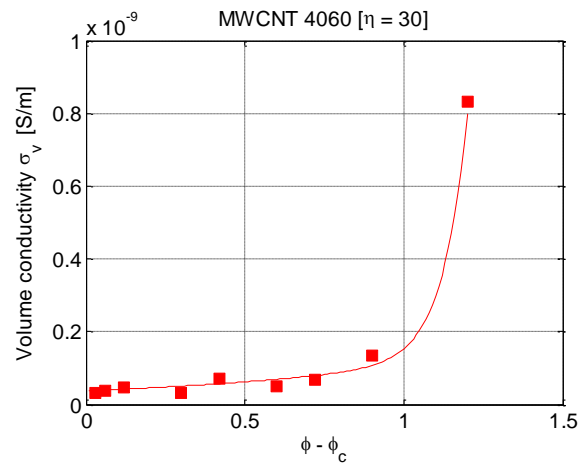


**Fig. 3.** Volume conductivity vs. MWCNT below the percolation threshold;  $\eta=30$

**Table 2.**

Percolation threshold vs. aspect ratio

aspect ratio $\eta$ [L/D]	30	105	667
percolation threshold $\phi_c$ [vol%]	$>1.5$	$\sim 0.42$	$\sim 0.42$
transition threshold $\phi$ [vol%]	//	$\sim 0.06$	$\sim 0.003$

### 3.2 Dielectric spectroscopy

Fig. 4 shows the variation of relative permittivity as a function of frequency of specimen filled with MWCNT at different concentrations and with different aspect ratios,  $\eta=30$  (Fig. 4a),  $\eta=105$  (Fig. 4b) and  $\eta=667$  (Fig. 4c). We explicitly remark that plots relative to composites

containing low filler content (i.e. <0.06% vol) are not shown since they do not differ sensibly from frequency spectra of the neat polymer shown in Fig. 5. Moreover, due to the high AC conductivity of the samples with filler content equal to 1.2% vol. and due to the limitations of the measuring equipment, it was not possible to measure the permittivity for these compositions.

The relative permittivity is strictly linked to the polarization in the material and it is related to the energy stored in the medium. This parameter usually depends from various contributions (interfacial, orientational, etc.) and, in particular, it can be strongly dependent on the eventual presence of crystalline phases in the host matrix, on the addition of fillers and on the frequency of the applied electric field. Usually the first two factors are responsible of typical interfacial phenomena best known as Maxwell-Wagner-Sillars (MWS) relaxations [17]. These effects, usually verified in heterogeneous systems subjected to periodical electric fields and particularly effective at low frequencies, are related to differences among permittivities and conductivities of different phases combined together rising, also in neat polymer matrices, from impurities and catalyst residues from the processing stage [18, 19].

Such a behavior is confirmed for the investigated systems since the dielectric constant increases remarkably with MWCNT concentration especially at low frequencies. This effect [20], particularly marked for systems above the percolation threshold, explained in terms of a gradual formation of micro-capacitor networks [20, 21] where many MWCNTs agglomerates are separated by very thin dielectric polymer layers.

At low frequencies (i.e. at 1 kHz, as shown in Fig. 6) and at low filler concentrations, far from the percolation threshold, the relative permittivity of the samples remains practically unchanged, almost equal to that of the neat resin ( $\epsilon_r=3.8$ ) while, with increasing MWCNTs content, the number of micro-capacitors increases and the insulation distance between them decreases, so that the capacitance of a single micro-capacitor increases.

In samples with  $\phi < \phi_c$ , relative permittivity sensibly increases above the percolation threshold  $\phi_c$  according to the following linear law:

Differently, in samples with  $\phi > \phi_c$  the threshold is not the percolation threshold, but the transition threshold  $\phi_t$ , above which relative permittivity changes linearly, with a much lower steepness, as:

The relative permittivity of all the test samples reaches a maximum at the highest volume content ; it is about  $\epsilon_r=55$  in samples with  $\eta=105$  and  $\eta=667$  while it assumes the value  $\epsilon_r=12.7$  in samples with  $\eta=30$ .

Such a behavior is not in contrast with percolation theory since the formation of a network of micro-capacitors is not a direct consequence of the formation of a conductive path between the electrodes. According to the authors opinion, this behavior deserves major attention, involving further investigations and the implementation of a suitable computer model, which is out of the scope of the present paper, in order to compare and validate experimental observations with numerical results.

As concerns the dependence on the applied frequency, in Fig. 4 it is shown that the relative permittivity decreases dramatically with frequency because it can be more difficult for larger dipolar groups to orient themselves and give their contribution to polarization. Such reduction is much sharper above the percolation threshold and it is almost negligible at low filler content. It is also interesting to observe that the marked decrease with frequency occurs at about 30 kHz in specimen with and at much higher frequency (about 2 MHz) in samples with , since the relaxation time is much greater for specimen containing nanotubes with higher aspect ratio.

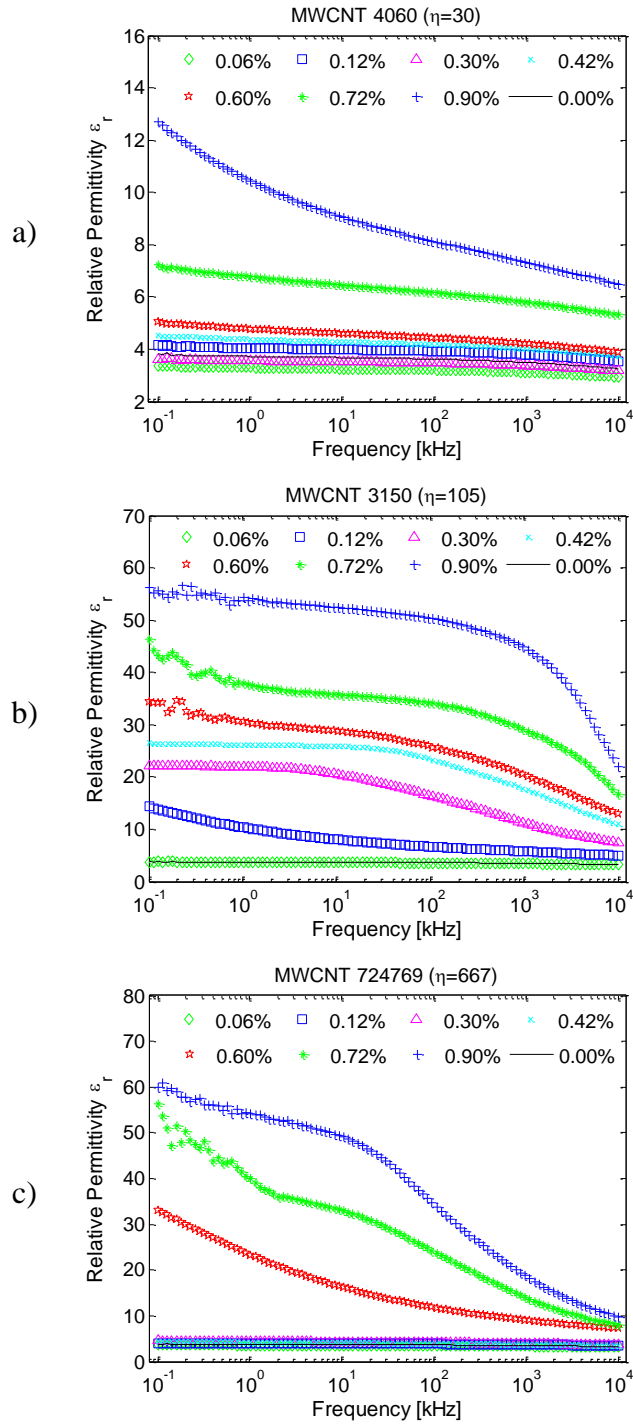


**Fig. 4.** Relative permittivity ( $\epsilon_r$ ) vs. frequency ( $f$ ) as a function at different filler content (vol%);

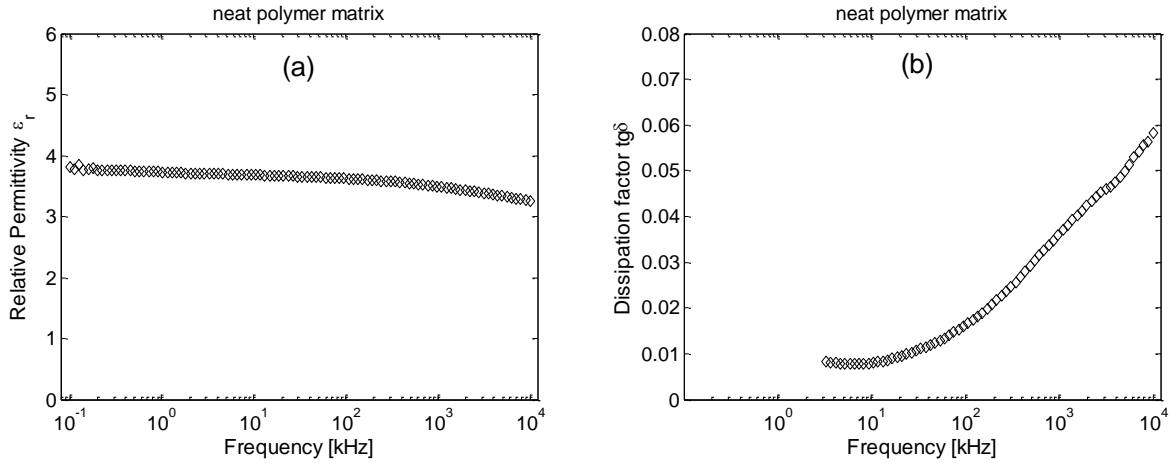


**Fig. 5.** Relative permittivity (a) and dissipation factor (b) vs. frequency ( $f$ ) for unfilled polymer;

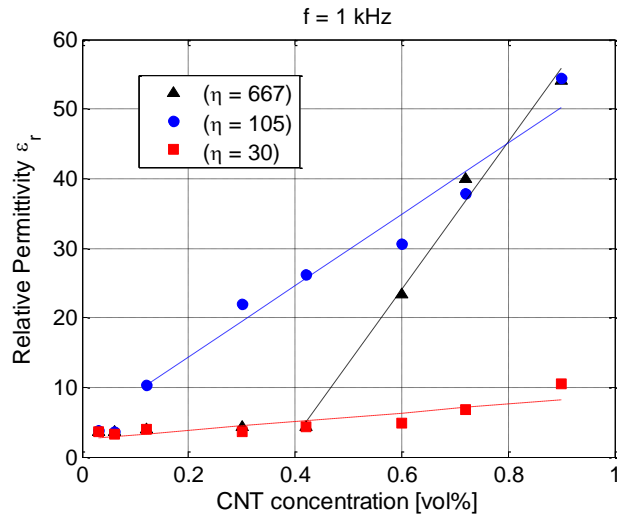


**Fig. 6.** Relative permittivity ( $\epsilon_r$ ) at 1 kHz vs. filler content at different aspect ratios  $\eta$ .

The frequency response of dissipation factor ( $tg\delta$ ) is shown in Fig. 7. The dissipation factor takes into account both conduction and polarization losses and it is strongly dependent on frequency, filler content and aspect ratio. The dissipation factor of the neat polymer is extremely low in all the measured frequency range; it increases with frequency and, in the measuring range, assumes its maximum ( ) at  $f=10$  MHz (Fig. 5b).

In composites with low aspect ratio (Fig. 7a), the variation of  $tg\delta$  with nanotube content is almost negligible, since the dissipation factor is always lower than 0.11. In samples with  $\eta=105$  (Fig. 7b) the dissipation factor remains practically unchanged at different filler concentrations and increases only above the percolation threshold. At low frequency it is possible to find an absorption phenomenon at high frequencies, caused by the orientation of dipolar groups. Similar

behavior can be observed in samples with  $\eta=667$  (Fig. 7c) in which the very high values of the dissipation factor ( ), assumed at low frequency and at high filler content, are the evidence of increasing conducting phenomena due to the presence of carbon nanotubes.

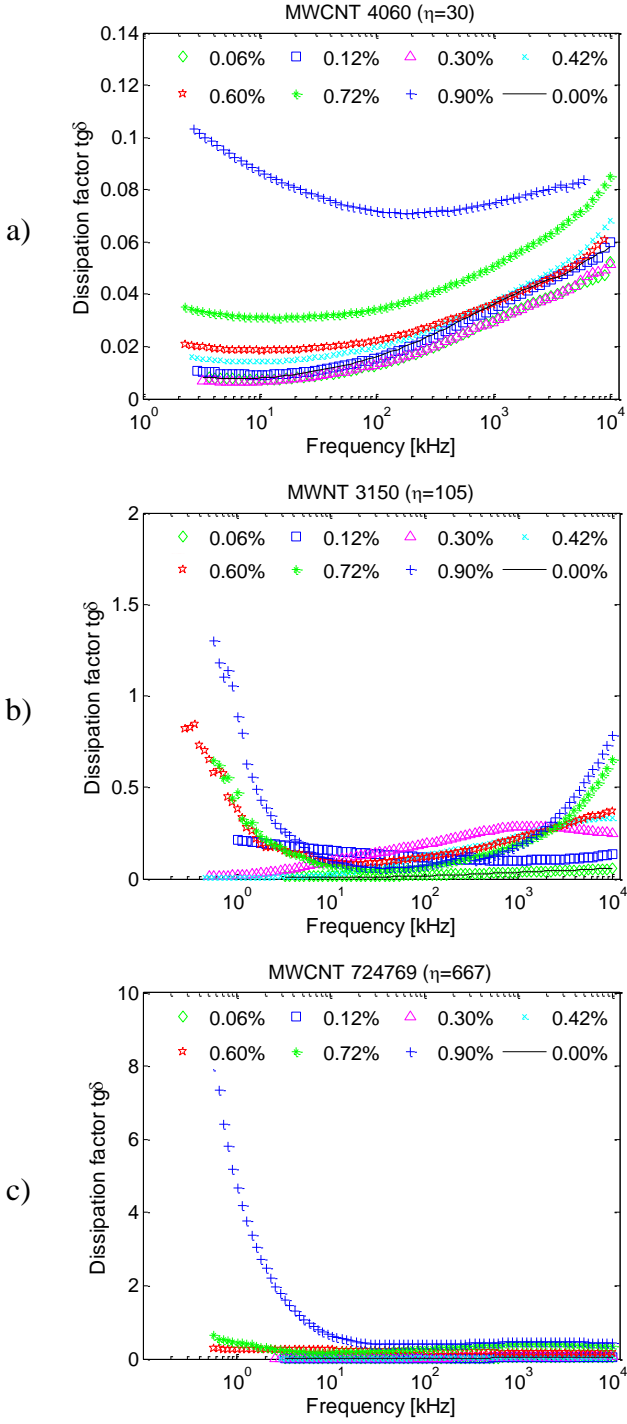


**Fig. 7.** Dissipation factor ( $tg\delta$ ) vs. frequency ( $f$ ) at different filler content (vol%)

### 3.4 Raman evidences

The Raman spectra of the investigated MWCNTs (see Fig. 8) display three prominent features: at  $1575\text{ cm}^{-1}$  we can find the G band, due to the tangential vibrations of the graphitic  $sp^2$  carbon atoms ( $E_{2g}$  symmetry). At  $1330\text{ cm}^{-1}$ , the so-called D (defect) band, originating from the breathing mode of the disordered graphite structure ( $A_{1g}$  symmetry) is observed; this peak reflects the presence of amorphous carbon mainly localized at the nanotube edges rather than defects in the tube walls [22-24]. A third feature is located at  $2670\text{ cm}^{-1}$ , with satellite components at  $2905$  and  $2415\text{ cm}^{-1}$ . This profile originates from second-order vibrational modes, in particular the overtone of the D fundamental [25]. In all spectra no radial bending modes are detected in the range  $100 - 300\text{ cm}^{-1}$  due to the hindrance exerted by the outer tubes on the breathing modes of the inner ones. By inspection of Fig. 8 it is apparent that MWCNT samples with aspect ratios ( $\eta$ ) equal to 105 and 667 are structurally equivalent, while the MWCNT sample 4060 with the lowest  $\eta$  shows distinct features. In particular, in the latter sample the D band is less prominent, indicating a reduced amount of amorphous phase with respect to the 724769 and 3150 samples. The structural regularity of MWCNTs is customary evaluated by the intensity ratio of the D- and G-lines: the  $I_D/I_G$  ratio is 0.47, 1.31 and 1.29 for 4060, 3150 and 724769 samples, respectively. The 64 % decrease of the disorder parameter for the 4060 sample is indicative of enhanced structural uniformity and highlights the more regular character of such samples with respect to that of the other two samples, which display essentially coincident characteristics. The trend of the  $I_D/I_G$  parameter is also consistent with the purity grade reported by the manufacturers (respectively, >97, >95, >95 %, see Table 1).

In light of the above considerations, the singular dielectric behavior shown by compounds filled with carbon nanotubes with the lowest aspect ratio can be attributed to the different behavior of this filler with respect to the ones characterized by higher  $\eta$  values. Both experimental and modeling activity is in progress in order to correlate the structural properties of the MWCNT with the electrical properties of the composites.



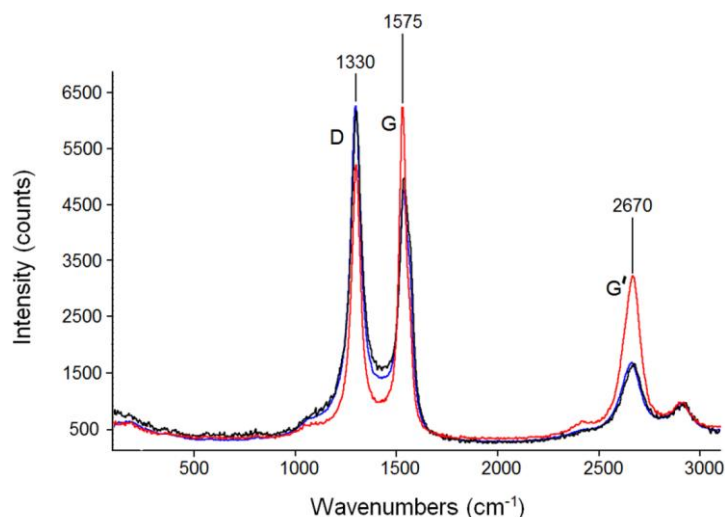


**Fig. 8.** Raman spectra of the MWCNTs: red trace: sample 4060; blue trace: sample 3150; black trace: sample 724769. The intensity scale refers to the red trace; the remaining spectra have been normalized with respect to the maximum intensity to facilitate the comparison.

### 3.4 Morphological aspects

As mentioned before, all compounds were systematically analyzed also to verify the level of dispersion of MWCNTs actually achieved under the applied processing conditions to prepare samples for dielectric tests.

At this regard, the highest magnification was limited by the electron-beam sensibility of the matrix. In fact, given that high acceleration voltages usually set to ensure high resolutions in SEM imaging of polymer matrices can lead to electron-beam damages, preliminary tests allowed to set the highest considerable magnification at 50.000 x.

Moreover, taking into account the high number of investigated compounds, for the sake of simplicity, morphological observations were performed only on samples with a filler content equal to 0.4 vol% (see Fig. 9).

Carbon nanotubes, clearly evident as emerging from the matrix in case of aspect ratio equal to 30 and bright dots as a result of their high electrical conductivity for higher aspect ratio, appear to be well dispersed with no big agglomerates in the nanocomposites. SEM pictures of all other examined compounds, herein not reported, allow to draw similar satisfying consideration about the achieved carbon nanotubes dispersion.

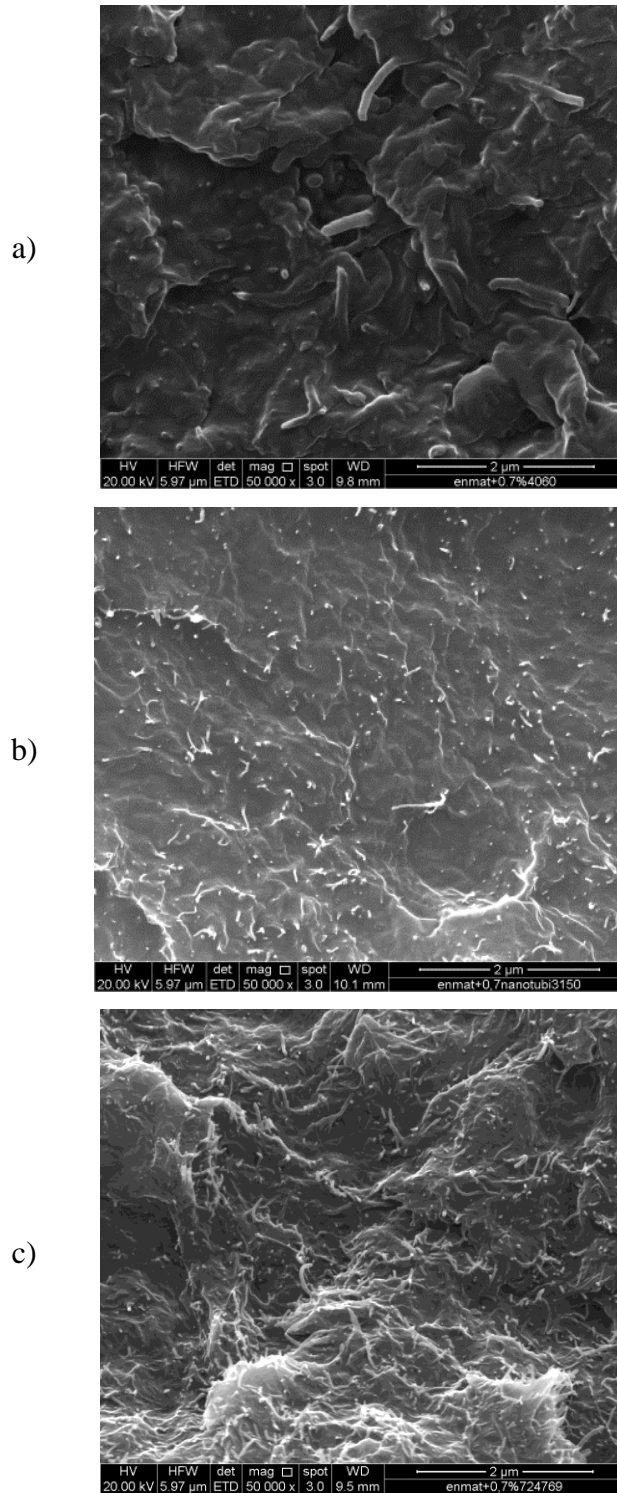


**Fig. 9.** SEM micrographs of cryofractured surfaces of samples containing 0.4 vol% of MWCTs with  $\eta$  equal to 30 (a), 105 (b) and 667 (c), respectively. Magnification: 50.000 x.

#### **4. Conclusions**

The dielectric behavior of a fully biodegradable commercial blend filled with multi wall carbon nanotubes was investigated as a function of filler content and aspect ratio. Melt compounded systems were systematically analyzed in terms of calorimetric properties, morphological aspects and, especially, of dielectric behavior to highlight any effect of the filler inclusion on the crystallinity of the matrix and dielectric parameters.

Results emphasized that the aspect ratio  $\eta$  of carbon nanotubes strongly influences the electrical properties of composites. High values of  $\eta$  enable electrical percolation of composites at low filler content; low frequency permittivity increases remarkably with MWCNT concentration in proximity of the percolation threshold; a maximum in dielectric losses can be found at a specific frequency and at a specific combination of filler content and aspect ratio.

#### **Acknowledgements**

This work has been partially supported by the POR Campania FSE 2007-2013 through the MASTRI (Materiali e Strutture Intelligenti) Project.

#### **References**

- [1] Pluta M, Galeski A, Alexandre M, Paul MA, Dubois P. Poly(lactide)/montmorillonite nanocomposites and microcomposites prepared by melt blending: structure and some physical properties. *J Appl Polym Sci* 2002;86:1497-1506.
- [2] Shibata M, Inoue Y, Miyoshi M. Mechanical properties, morphology, and crystallization behavior of blends of poly(l-lactide) with poly(butylene succinate-co-l-lactate) and poly(butylenes succinate). *Polymer* 2006;47:3557-3564.
- [3] Bruzaud S. Polyhydroxyalkanoates-based nanocomposites: an efficient and promising way of finely controlling functional material properties. In: J.K. Pandey et al. Eds. *Handbook of polymernanocomposites. Processing, performance and application, Volume A: Layered Silicates*. 2014. p. 1-20.
- [4] Scaffaro R, Dintcheva NTz, Marino R, La Mantia FP. Processing and properties of biopolymer/polyhydroxyalkanoates blends. *J Polym Environ* 2012;20:267-272.

- [5] Munoz-Bonilla A, Cerrada ML, Fernandez-Garcia Marta, Kubacka A, Ferrer M, Fernandez-Garcia Marcos. Biodegradable polycaprolactone-titania nanocomposites: preparation, characterization and antimicrobial properties. *Int J Mol Sci* 2013;14:9249-9266.
- [6] Campos A, Marconcini JM, Imam SH, Klameczynski A, Ortis WJ, Wood DH, Williams TG, Martins-Franchetti SM, Mattoso LHC. Morphological, mechanical properties of biocomposite thermoplastic starch and polycaprolactone reinforced with sisal fibers. *J Reinf Plast Comp* 2012;31:573-581.
- [7] Potschke P, Paul DR. Formation of co-continuous structures in melt-mixed immiscible polymer blends. *J Macromol Sci Part C: Polymer Rev.* 2007;43:87-141.
- [8] Filippone G, Dintcheva NTz, Acierno D, La Mantia FP. The role of organoclay in promoting co-continuous morphology in high density poly(ethylene)/poly(amide) 6 blends. *Polymer.* 2008;49:1312-1322.
- [9] Javadi A, Kramschuster AJ, Pilla S, Lee J, Gong S, Turng LS. Processing and characterization of microcellular PHBV/PBAT blends. *Polym Eng Sci.* 2010;50: 1440-1448.
- [10] Nagarajan V, Misra M, Mohanty AK. New engineered biocomposites from poly(3-hydroxybutyrate-co-3-hydroxyvalerate) (PHBV)/ poly(butylene adipate-co-terephthalate) (PBAT) blends and switchgrass: fabrication and performance evaluation. *Ind Crop Prod.* 2013; 42:461-468.
- [11] Li J, Ma PC, Chow WS, To CK, Tang BZ, Kim JK. Correlations between percolation threshold, dispersion state, and aspect ratio of carbon nanotubes. *Adv Funct Mater.* 2007;17:3207-3215.
- [12] Lu C, Mai YW. Influence of aspect ratio on barrier properties of polymer-clay nanocomposites. *Phys Rev Lett.* 2005;95:88303-1 – 88303-4.
- [13] Bauhofer W, Kovacs JZ. A review and analysis of electrical percolation in carbon nanotube-based composites. *Comp Sci Techn.* 2009;69:1486-1498.
- [14] Kim HS, Park BH, Yoon JS, Jin HJ. Thermal and electrical properties of poly (l-lactide)-graft-multiwalled carbon nanotube composites. *Eur Polym J.* 2007;43:1729-1735.
- [15] Balberg I, Anderson CH, Alexander S, Wagner N. Excluded volume and its relation to the onset of percolation. *Phys Rev B.* 1984;30:3933-3943.

- [16] Alig I, Pötschke P, Lellinger D, Skypa T, Pegel S, Kasaliwal GR, Villmow T. Establishment, morphology and properties of carbon nanotube networks in polymer melts. *Polymer*. 2012;53:4 – 28.
- [17] R. Bartnikas, R.: Eichhorn, *Engineering Dielectrics Volume IIA Electrical Properties of Solid Insulating Materials: Molecular Structure and Electrical Behavior*, ASTM, 1983
- [18] Perrier G, Bergeret A. Maxwell-Wagner-Sillars relaxations in polystyrene-glass bead composites. *J Appl Phys*. 1995;77:2651-2658.
- [19] Arous M, Hammami H, Lagache M, Kallel A. Interfacial polarization in piezoelectric fibre-polymer composites. *J Non-Cryst Solids*. 2007;353:4428-4431.
- [20] Q. Li, Q. Xue, L. Hao, X. Gao, Q. Zhehg, Large dielectric constant of the chemically functionalized carbon nanotube/polymer composites, *Composites Science and Technology*, Vo. 68, pp. 2290-2296, 2008
- [21] Ahmad K, Pan W, Shi SL. Electrical conductivity and dielectric properties of multiwalled carbon nanotube and alumina composites. *Appl Phys Lett*. 2006;89:133102-1-3.
- [22] Saito R, Jorio A, Souza Filho AG, Dresselhaus G, Dresselhaus MS, Pimenta MA. Probing phonon dispersion relations of graphite by double resonance Raman scattering. *Phys Rev Lett* 2001;88(2):027401-1–4.
- [23] Osswald S, Flahaut E, Ye H, Gogotsi Y. Elimination of D-band in Raman spectra of double-wall carbon nanotubes by oxidation. *Chem Phys Lett* 2005;402(4–6):422–7.
- [24] Bose SM, Gayen S, Behera SN. Theory of the tangential Gband feature in the Raman spectra of metallic carbon nanotubes. *Phys Rev B* 2005;72(15):153402-1–4.
- [25] Chakrapani N, Curran S, Bingqing W, Ajayan PM, Carrillo A, Kane RS. Spectral fingerprinting of structural defects in plasma-treated carbon nanotubes. *J Mater Res* 2003;18(10):2515–21.
- [26] ~~Kim KK, Park JS, Kim SJ, Geng HZ, An KH, Yang C M, et al. Dependence of Raman spectra G0 band intensity on metallicity of single wall carbon nanotubes. *Phys Rev B* 2007;76(20):205426-1–8.~~